Pulse Gas Injection in Separation Zone of Hypersonic MHD Flow Over Rotation Body

E. Gubanov, A. Likhachev, and S. Medin

Introduction

In our previous studies [1, 2], we modeled the hypersonic magnetohydrodynamic (MHD) flow over rotation bodies with imbedded magnetic dipole. The simulations were conducted in the framework of the complete MHD model considering viscosity, thermal conductivity, induced magnetic field, and real-air thermodynamic properties. It was revealed that the MHD interaction can lead to the formation of extensive separation zones with practically motionless medium. The gasdynamic streamlines bypass the separation zone following close to magnetic lines of force. The position and size of the separation zones at the body surface depend on and are controlled by the direction and value of the dipole magnetic moment. It was revealed that the surface heat flux inside this zone is markedly reduced. It is of interest to consider the possibilities of additional heat protection of the body surface by a cold gas pulse injection to the separation zone which looks quite stable against external impacts. This is the problem considered in the present paper by means of the numerical modeling. The study is conducted using the same physical model as in [1, 2].

Problem Formulation

The problem is considered in two formulations. *In the first of them* (*A*), the body is the cylinder of circular cross section with axis perpendicular to the incident flow velocity vector. To reduce the problem to the 2D formulation, the cylinder is supposed to be infinite. Two parallel wires are disposed inside the cylinder. The currents in the wires flow in opposite directions. The dipole magnetic moment is normal to the incident flow velocity vector as well as to the cylinder axis. The problem is considered in cylindrical coordinate system, the axis z of which coincides with the cylinder axis (Fig. 1). The diameter of the cylinder is equal to 4 m; the distance between wires is 2 m. The incident flow parameters are taken as follows: velocity $v_1 = 7 \times 10^3$ m/s, pressure $p_1 = 10$ Pa, and density $\rho_1 = 1.765 \times 10^{-4}$ kg/m^3. The values of pressure and density are close to the Earth atmosphere parameters at the altitude of 65 km. The total magnetic field $\boldsymbol{B}$ is a superposition of the dipole ($\boldsymbol{B_d}$) and the induced ($\boldsymbol{B_i}$) magnetic fields. The dipole magnetic field $\boldsymbol{B_d}$ is the two-component vector $\boldsymbol{B_d} = B_{dr}\boldsymbol{e}_r + B_{d\theta}\ \boldsymbol{e}_\theta$ calculated in accordance with the Biot–Savart law. The wire current I_w is equal to 2×10^7 A. In this formulation the problem is two-dimensional and may be solved in half-plane r–θ. The computations have been performed in the half-ring domain of width AB = DE = 40 m within the interval of angle θ from 0 to π.

To solve the problem numerically, the stabilization method with splitting of the complete equation system into electrodynamic and gasdynamic subsystems is used. The induction equation is solved to find the induced magnetic field; the Maxwell equations are used to reconstruct other electrodynamic parameters. The flow parameters are found from the solution of the Navier–Stokes equations with the MHD source terms. It is assumed that the air medium is thermodynamically equilibrium; the radiative heat transfer and the Hall effect are neglected. The thermodynamic properties are determined in accordance with [3]; transport coefficients were computed using the well-proven codes [4]. The second-order total variation diminishing (TVD) scheme with upwind differences [5] generalized to an arbitrary equation of state [6] has been used to solve the gasdynamic subsystem. The terms of the equations associated with viscosity and heat conductivity have been approximated in a standard second-order symmetric scheme. The codes solving the induction equation have been realized on the base of the numerical scheme [7]. The computations

E. Gubanov • A. Likhachev (✉) • S. Medin
Joint Institute for High Temperatures, Russian Academy of Sciences, Izhorskaya Street 13 Bd. 2, Moscow 125412, Russia
e-mail: apl@ihed.ras.ru

G. Ben-Dor et al. (eds.), *30th International Symposium on Shock Waves 2*, DOI 10.1007/978-3-319-44866-4_2

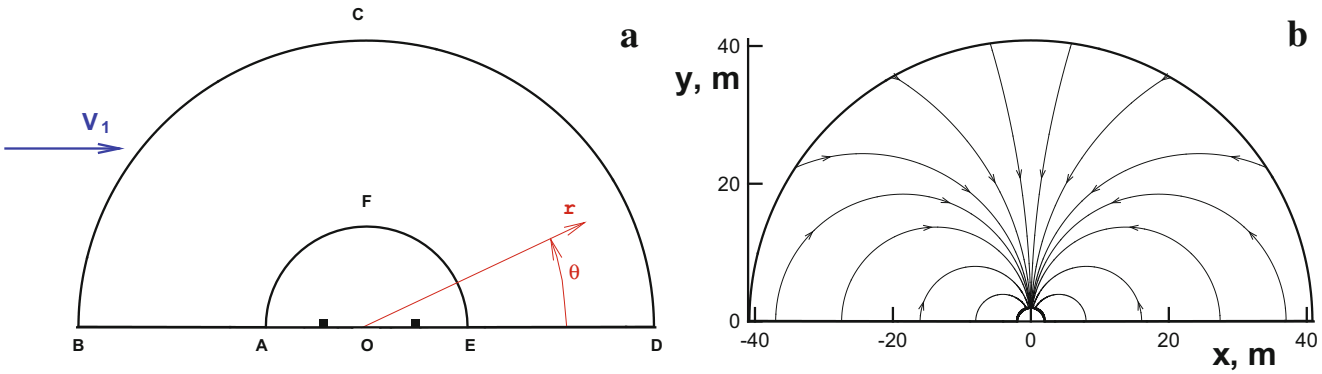

Fig. 1 Formulation A: flow scheme (**a**) and lines of force of the dipole magnetic field (**b**). The positions of wires are shown by small black squares on the segment AE (**a**)

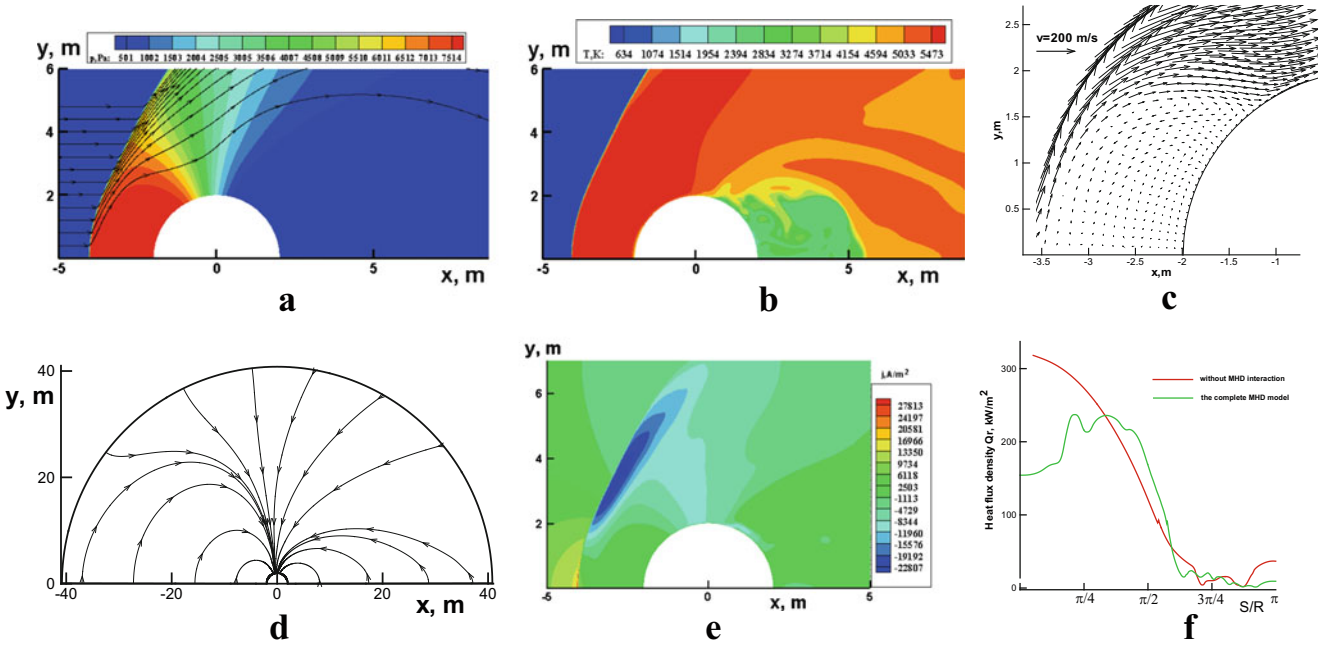

Fig. 2 The initial conditions in formulation A: pressure distribution and streamlines (**a**), temperature field (**b**), fragment of velocity vector diagram (**c**), lines of force of the total magnetic field (**d**), distribution of the current density component j_z (**e**), and wall heat flux density profiles along coordinate S/R (**f**). Here and below the distance S is counted along the body boundary from the front critical point; R is the body radius

have been performed on multiprocessor computer systems using the MPI parallel programming technology.

Incident flow parameters $v_r = v_1 \cos\theta$, $v_\theta = -v_1 \sin\theta$, $p = p_1$, and $\rho = \rho_1$ are set at the boundary BC. The "soft" boundary condition $\partial/\partial n = 0$ is used at the boundary CD. The symmetry condition is given at the boundaries AB and DE. The equal-zero condition for normal and tangential velocity components is used at the cylinder boundary AFE with the exception of the injection place and time. The temperature of the cylinder surface is constant and equal to 2000 K. The boundary conditions for the induced magnetic field are the following: the "soft" conditions are used on boundaries BC and CD; the symmetry conditions are assigned on boundaries AB and DE. The body electric conductivity is zero, so that the numerical cells inside sphere have been excluded from calculations. The zero electric field E_z has been assigned on the cylinder surface.

The stationary solution of the above-formulated problem without injection (Fig. 2) is used as initial conditions to model unsteady MHD flow initiated by the cold gas pulse injection.

The pulse injection of the cold gas into the separation zone is performed through the cylinder surface segment in the angle interval $2.74 < \theta < 3.14$ with parameters $v_{r\ \mathrm{in}} = 300$ m/s, $v_{\theta\ \mathrm{in}} = 0$, $p_{\mathrm{in}} = 7700$ Pa (this value is approximately equal to the pressure near the front critical point in

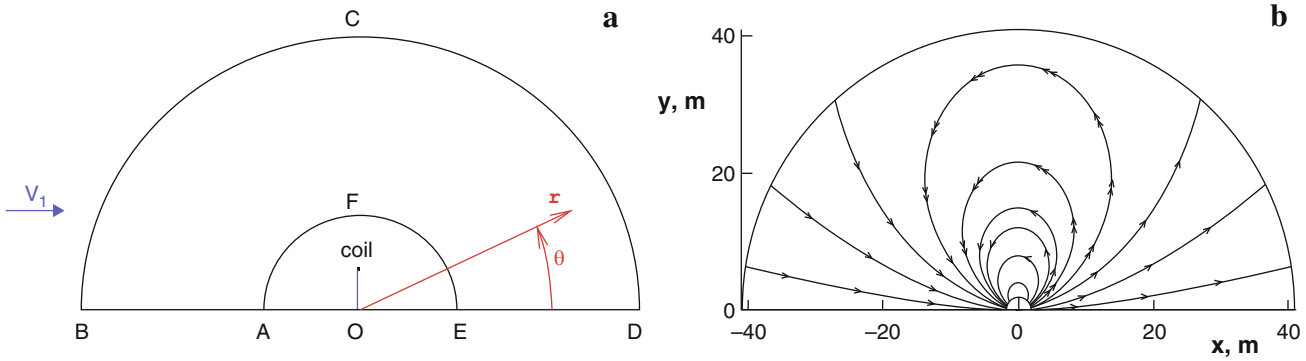

Fig. 3 Formulation B: flow scheme (**a**) and lines of force of the dipole magnetic field (**b**). As in formulation A, the stationary solution of the problem without injection is used as initial conditions (Fig. 4)

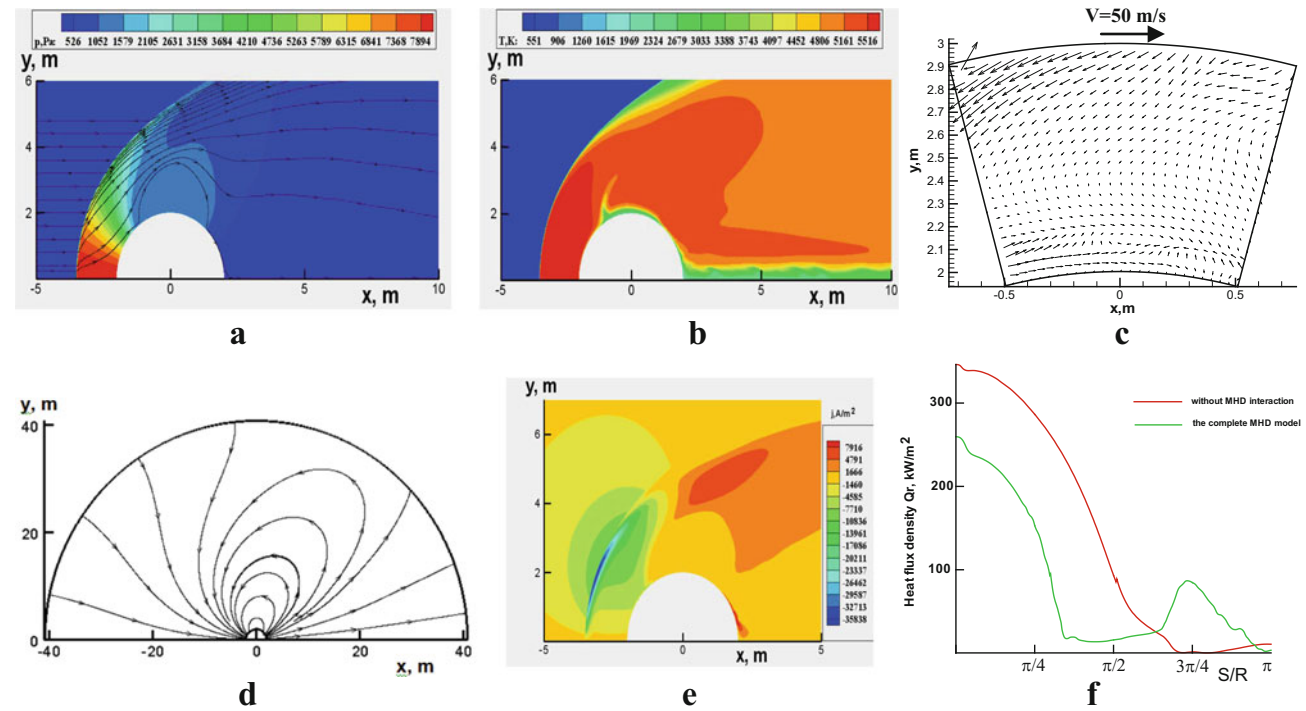

Fig. 4 The initial conditions in formulation B: pressure distribution and streamlines (**a**), temperature field (**b**), fragment of velocity vector diagram (**c**), lines of force of the total magnetic field (**d**), distribution of the current density component j_φ (**e**), and wall heat flux density profiles along coordinate S/R (**f**)

the solution without injection), $\rho_{in} = 13.4 \times 10^{-3}$ kg/m^3, and $T_{in} = 2000$ K equal to the wall temperature. The injection duration is 5 ms; the injected gas mass is 0.032 kg per running meter along the cylinder.

The second formulation (*B*) is close to the above described except that the body is a sphere and the dipole magnetic field is generated by current flowing in the ring coil disposed inside the sphere. The centers of the sphere and the coil coincide. The dipole magnetic moment is directed along the incident flow velocity vector. The problem is considered in spherical coordinate system rigidly bound with the sphere. The origin is located at the sphere center (Fig. 3). The sphere diameter is equal to 4 m; the coil diameter is 2 m. The problem is two-and-half dimensional and may be solved in half-plane r–θ. The computations have been performed in the half-ring domain of width AB = DE = 40 m within the range of angle θ from 0 to π. The injection is performed through the body boundary in the angle interval $1.3 < \theta < 1.7$ with parameters $v_{r\ in} = 300$ m/s, $v_{\theta\ in} = 0$, $p_{in} = 1130$ Pa, $\rho_{in} = 1.965 \times 10^{-3}$ kg/m^3, and $T_{in} = 2000$ K. The injected gas mass is 0.029 kg. Other model assumptions and parameters are the same as those in formulation A (Fig. 4).

Results and Discussion

The flow features after the injection *in formulation A* are illustrated by Figs. 5 and 6. As is seen from Fig. 5, the injection initiates a complicated vortex flow in the separation zone (more exactly, the zone of the flow pushing out) in front of the body. The intensity of vortices decreases rapidly with time, and after 15 ms, the only vortex of decreasing strength remains. The injected gas cools the shock layer plasma and partially displaces it to the external flow. The plasma mass in the separation zone before the injection is 0.014 kg per running meter and becomes near 0.025 kg per running meter after 20 ms upon its completion (remind that the injected gas mass is 0.032 kg per running meter). It is seen that the separation zone is not destroyed, in general maintaining its configuration, although the injection was rather intensive.

As follows from the comparison of Figs. 2f and 6a, the injection leads to a sharp decrease of heat flux densities at the upstream cylinder surface. It is of importance that the integral cooling effect is clearly pronounced and remains much longer than the injection time (Fig. 6b). The pulse cold gas injection may be repeated with needed frequency to support this effect on the desired level.

Figures 7 and 8 illustrate the unsteady flow characteristics *in formulation B*.

The plasma mass in the separation zone before the injection is 0.025 kg and becomes near 0.036 kg after 40 ms upon its completion (remind that the injected gas mass is 0.029 kg). As in formulation A, the injection has rather strong impact on the separation zone initiating the formation of vortices and partial displacement of plasma from this zone to the external flow (Fig. 7). At the same time, the intensity of vortices quickly decreases with time, and flow topology remains resistant to the injection influence. As follows from the comparison of Figs. 4f and 8a, the injection results in a decrease of heat fluxes on the side and downstream body surfaces. It is of importance that the integral cooling effect is clearly pronounced and remains much longer than the injection time, but its value is less than that in formulation A (Fig. 8b). This is because surface heat fluxes in front of the body, being the bulk of the total heat flux, are practically independent of the injection to the separation zone located on the side sphere surface.

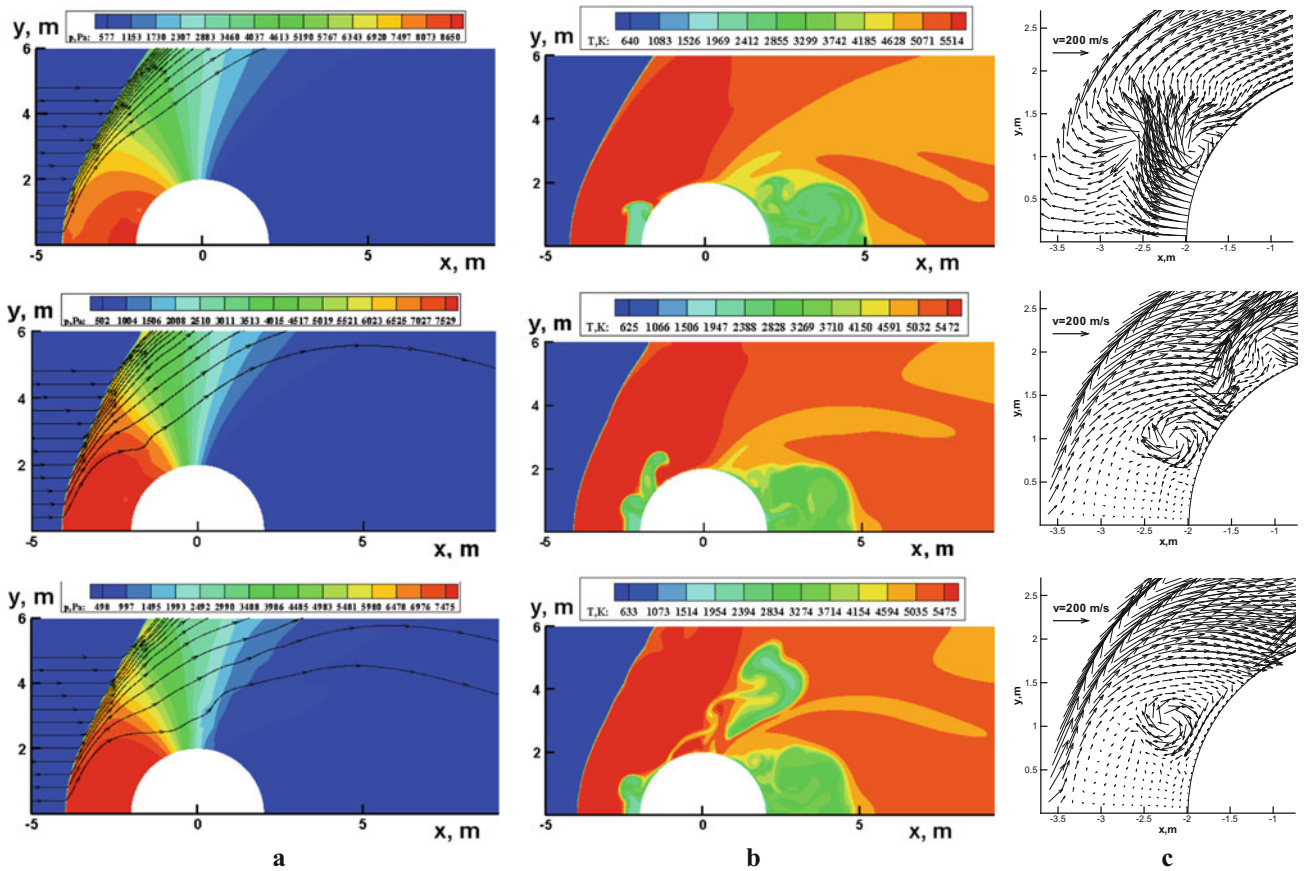

Fig. 5 The evolution of the flow over the cylinder at the three moments of time after injection completion: 0 ms (*upper row*), 12 ms (*middle row*), and 17 ms (*lower row*). Pressure and streamlines (**a**), temperature (**b**), and fragment of velocity vector diagram (**c**) are shown in every row

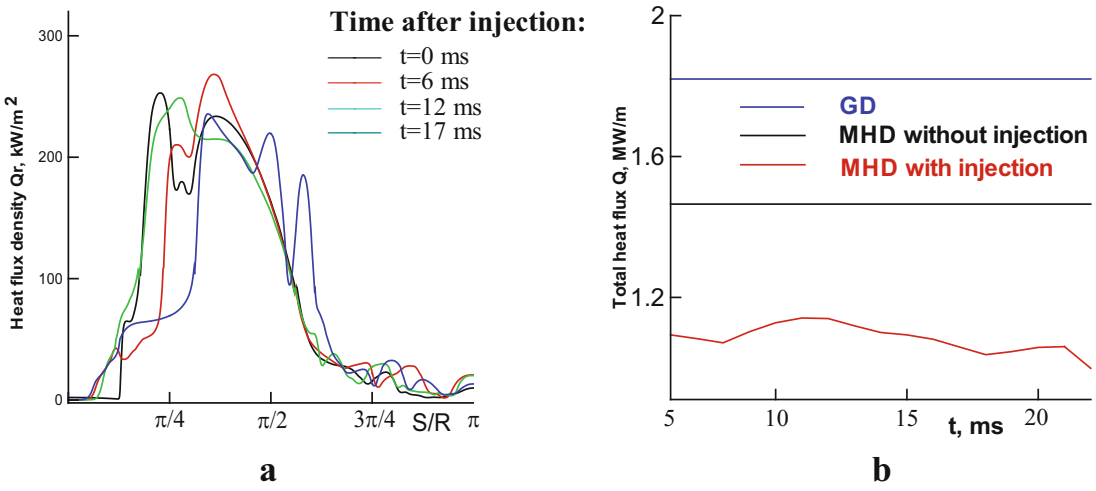

Fig. 6 The wall heat flux density profiles along coordinate *S*/*R* at different moments of time (**a**) and the time dependence of the total heat flux per running meter into the body for different physical conditions (**b**)

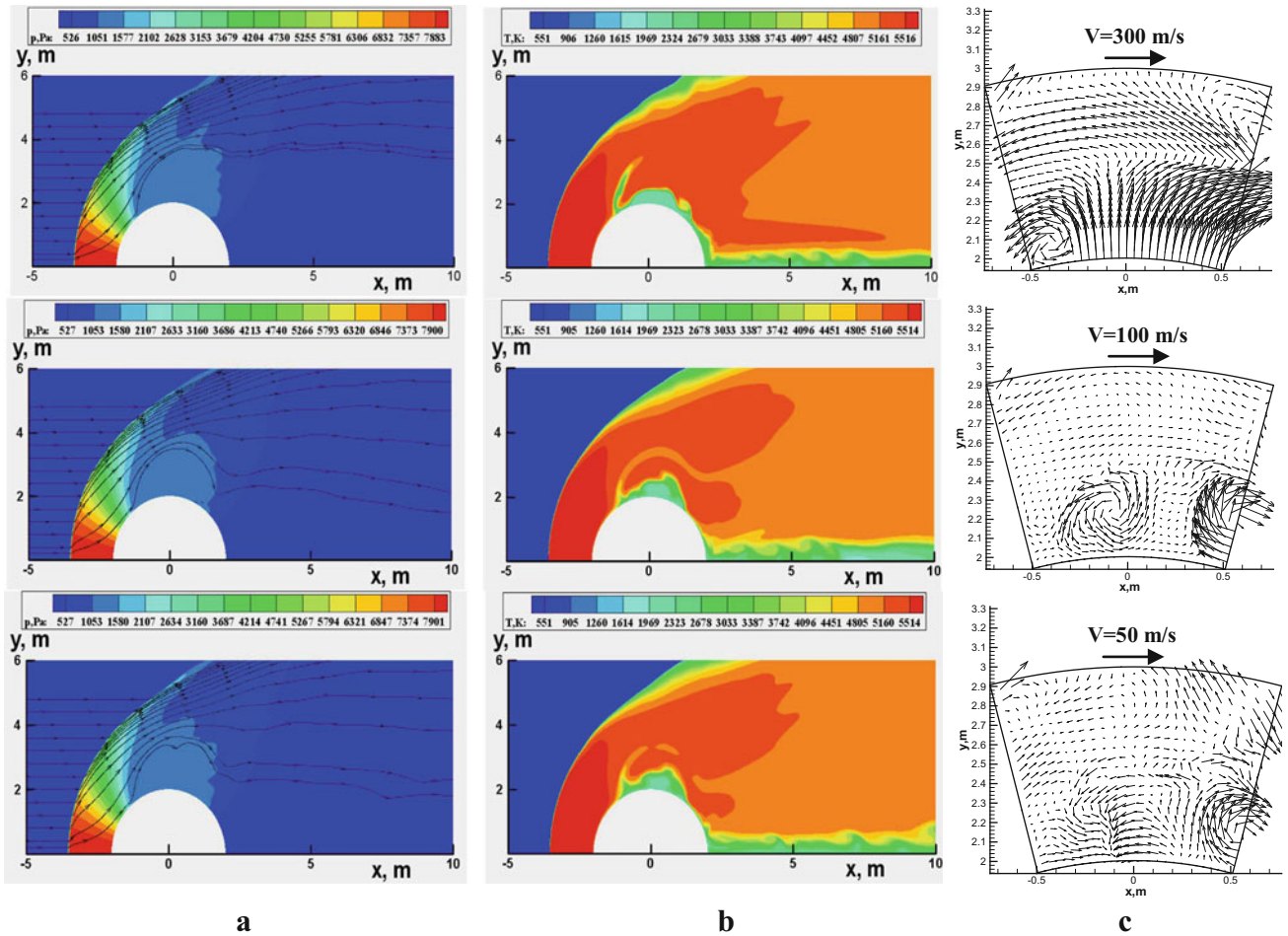

Fig. 7 The evolution of the flow over the sphere at the three moments of time after injection completion: 0 ms (*upper row*), 18 ms (*middle row*), and 36 ms (*lower row*). Pressure and streamlines (**a**), temperature (**b**), and fragment of velocity vector diagram (**c**) are shown in every row

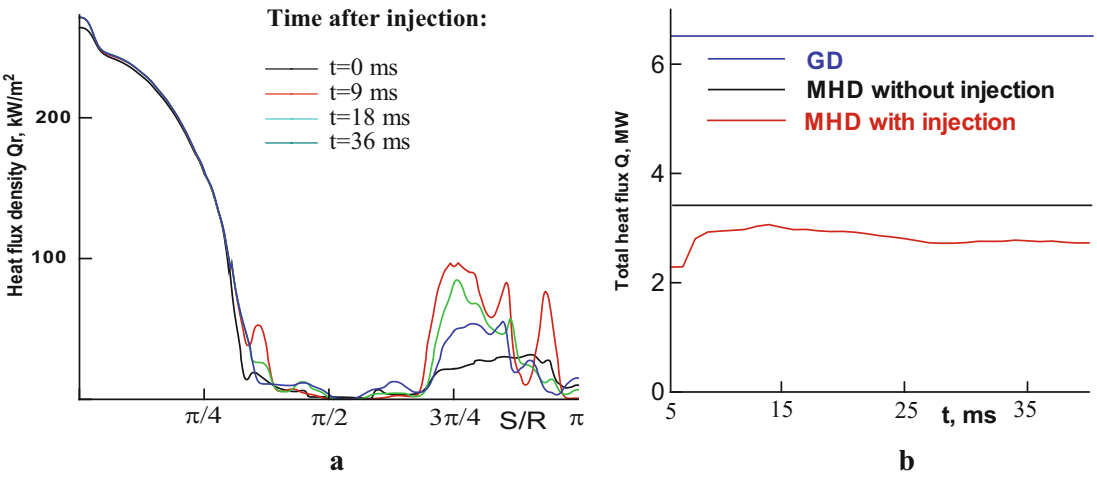

Fig. 8 The wall heat flux density profiles along coordinate *S*/*R* at different moments of time (**a**) and the time dependence of the total heat flux into the body for different physical conditions (**b**)

The fact that the cold gas is injected precisely into the separation zone plays a fundamental role in the cooling effect observed. Control calculations of the injection into the shock layer not discussed here due to lack of space show that the injected gas is immediately blown off downstream, and the integral cooling effect is observed during the injection time only. Moreover, the injected gas flow destroys the separation zone on the side sphere surface resulting in the increase of the total heat flux during long time after injection.

Conclusions

In the present study, it has been shown that the injection of cold gas into the separation zones leads to cooling of this region and the corresponding decrease of the total heat flux. The effect persists for a long time after the injection termination. It is shown that this effect does not depend on the separation zone location but manifests itself more intensively in the case of the injection into the separation zone in the shock layer.

In connection with the presented results, a number of interesting questions arise. In particular, the magnetic Reynolds number in the simulated MHD flows is near 10^{-1}, and the influence of induced magnetic field on the phenomena studied is rather weak. Yet the magnetic field in both formulations is markedly deformed (compare Figs. 1b, 3b and Figs. 2d, 4d). If flight conditions are characterized by essentially higher magnetic Reynolds numbers, the separation zone structure is expected to be more resistant to the cold gas injection and the cooling effect may be more substantial.

The radiative heat transfer is not considered in this work although it is of importance in the hypersonic aerodynamics. One can suppose that the injection of the optically dense gas with the needed pulse frequency may be helpful to mitigate this problem.

Of course, these and other accompanying questions require special consideration.

Acknowledgments The work was carried out with financial support from the Russian Foundation for Basic Research (Project No. 15-08-01687).

References

1. Gubanov, E.V., Likhachev, A.P., Medin, S.A.: Hypersonic MHD flow over rotation body at finite magnetic Reynolds numbers. In: Bityurin, V.A. (ed.) Proceedings of the 10th International WS on Magneto-Plasma Aerodynamics, Moscow, Russia, pp. 342–348, 22–24 March 2011
2. Gubanov, E.V., Likhachev, A.P., Medin, S.A.: On the sphere MHD overflow with separation zones at finite magnetic Reynolds numbers. In: Bityurin, V.A. (ed.) Proceedings of the 11th International WS on Magneto-Plasma Aerodynamics, Moscow, Russia, pp. 312–319, 10–12 April 2012
3. Kraiko, A.N., Makarov, V.E.: Explicit analytic formulas defining the equilibrium composition and thermodynamic functions of air for temperatures from 200 to 20,000 K. High Temp. **34**(2), 202–213 (1996)
4. Ivanov, P.P.: Mathematical modeling of perspective heat balance diagrams of power generation systems (in Russian). Preprint No 3-47, JIHT of RAS, Moscow (2004)
5. Harten, A.: High resolution schemes for hyperbolic conservation laws. J. Comput. Phys. **49**(2), 357–393 (1983)
6. Glaister, P.: An approximate linearized Riemann solver for the Euler equations for real gases. J. Comput. Phys. **74**(2), 382–408 (1988)
7. Gubanov, E.V., Likhachev, A.P., Medin, S.A.: MHD effects in the interaction of a meteoroid with planetary envelopes (in Russian). Preprint No. 3-428, JIHT of RAS, Moscow, (1999)

http://www.springer.com/978-3-319-44864-0

30th International Symposium on Shock Waves 2
ISSW30 - Volume 2
Ben-Dor, G.; Sadot, O.; Igra, O. (Eds.)
2017, XXXI, 742 p. 704 illus., 355 illus. in color.,
Hardcover
ISBN: 978-3-319-44864-0